

Theoretical Analysis of Dilepton Spectra in Heavy Ion Collisions at GSI-FAIR Energies

Diana Schumacher, Sascha Vogel and Marcus Bleicher

Institut für Theoretische Physik,
Johann Wolfgang Goethe-Universität, Frankfurt am Main,
D-60438 Frankfurt am Main, Germany

Received 1 January 2004

Abstract. This paper addresses the theoretical analysis of dilepton spectra in C+C collisions at GSI-SIS energies. Theoretical predictions for the recent data of the HADES collaboration at SIS-energies are made with the help of a hadron-string transport model, the Ultra-relativistic Quantum Molecular Dynamics (UrQMD) model. A mass shift of the ρ meson due to kinematical effects is discussed.

Keywords: dileptons, SIS, UrQMD, HADES
PACS: 13.40.Hq, 24.10.Lx, 25.75.-q, 25.75.Dw

1. Introduction

Dilepton spectra are expected to play an important role in indicating deconfinement and the restoration of the spontaneous breaking of chiral symmetry. Particularly in the low mass region, dileptons couple directly to light vector mesons and can therefore reflect the mesons mass distribution in the hot and dense region. Since dileptons do not interact strongly with the surrounding hadronic medium, they escape the fireball of a heavy ion collision and might carry information on properties of the early stage of the collision. Thus, they are one of the most crucial observables for the exploration of the QCD mass generation [1, 2, 3, 4, 5].

Heavy ion reactions with energies around 1 – 2 AGeV create a reaction zone of high nuclear density for about 10 fm/c. This is long compared to the typical lifetime of a hadronic resonance. Thus, the ρ -mesons with lifetimes of $\tau \simeq 1$ fm/c, can decay within this zone and the decay products (i.e., the e^+e^- -pairs) still carry the properties of the dense medium. The ω meson ($\tau \simeq 22$ fm/c) and the ϕ meson ($\tau \simeq 44$ fm/c) have longer lifetimes and can therefore escape the fireball before

they decay. Consequently, the ρ meson is the most prominent candidate to study in-medium modifications of hadron properties in high density nuclear collisions.

Calculations at low beam energies fall in the category of non-perturbative QCD, i.e., no exact methods to solve the equations of motion at QCD exist. Therefore one is forced to utilise approximations within effective field theories and compare with the results of experiments. In this paper, we focus on the HADES experiment at GSI-SIS [6].

For our studies we apply the UrQMD model. It is a non-equilibrium transport approach based on the covariant propagation of hadrons and strings. All cross sections are calculated by the principle of detailed balance or are fitted to available data. The model allows to study the full space time evolution for all hadrons, resonances and their decay products. This permits to explore the emission patterns of the resonances in detail and to gain insight into the origin of the resonances. UrQMD has been successfully applied to study light and heavy ion reactions at SIS. Detailed comparisons of UrQMD with a large body of experimental data at SIS energies can be found in [7]. For further details of the model the reader is referred to [8, 9].

2. Theoretical Background for Dilepton Production

2.1. Dalitz Decay of π^0 , η , ω and η'

Here, we follow [10] and [11] to derive the equations for the decay rate of a meson into dileptons. In general, these processes have the form

$$P \rightarrow V e^+ e^-, \quad V \rightarrow P e^+ e^-, \quad (1)$$

with P being a pseudoscalar meson and V being a vector meson. These processes are not true three-body decays because the processes can be split into two subprocesses. Thus, the decay $A \rightarrow B e^+ e^-$ can be separated into the decay of a virtual photon, $A \rightarrow B \gamma^*$, which subsequently decays via electromagnetic conversion, $\gamma^* \rightarrow e^+ e^-$. According to [10] and [11] we arrive at the Dalitz decay formulas, which differ only in the values for the form factors and if the particle B is a real photon ($m_B = 0$) or a virtual photon ($m_B \neq 0$):

- Dalitz decay of the pseudoscalar mesons π^0 , η and η' ($m_B = 0$):

$$\begin{aligned} \frac{dN_{A \rightarrow \gamma e^+ e^-}}{dM} &= \frac{4\alpha}{3\pi M} \sqrt{1 - \frac{4m_e^2}{M^2}} \left(1 + \frac{2m_e^2}{M^2}\right) \left(1 - \frac{M^2}{m_A^2}\right)^3 \\ &\times |F_{AB}(M^2)|^2 \frac{\Gamma_{A \rightarrow 2\gamma}}{\Gamma_{tot}} \langle N_A \rangle. \end{aligned} \quad (2)$$

The quantity $\langle N_A \rangle$ is the number of mesons A per event, M is the invariant mass of the lepton pair, m_e the electron mass, and F_{AB} the corresponding form factor.

- Dalitz decay of the vector meson ω ($m_B \neq 0$):

$$\begin{aligned} \frac{dN_{A \rightarrow B e^+ e^-}}{dM} &= \frac{2\alpha}{3\pi M} \sqrt{1 - \frac{4m_e^2}{M^2}} \left(1 + \frac{2m_e^2}{M^2}\right) |F_{AB}(M^2)|^2 \frac{\Gamma_{A \rightarrow 2\gamma}}{\Gamma_{tot}} \langle N_A \rangle \\ &\times \left(\left(1 + \frac{M^2}{m_A^2 - m_B^2}\right)^2 - \left(\frac{2m_A M}{m_A^2 - m_B^2}\right)^2 \right)^{3/2}. \end{aligned} \quad (3)$$

The Dalitz decay of the Δ resonance, $\Delta \rightarrow N e^+ e^-$, differs from the previous discussed decays because of the different interaction $N\Delta\gamma$ vertex. The decay rate reads as follows

$$\frac{dN_{e^+ e^-}}{dM} = \int \frac{dN_{\Delta \rightarrow N e^+ e^-}(M_\Delta)}{dM} \frac{dN_\Delta}{dM_\Delta} dM_\Delta = \int \frac{2\alpha}{3\pi M} \frac{\Gamma(M_\Delta, M)}{\Gamma_{\Delta 0}^{tot}} \frac{dN_\Delta}{dM_\Delta} dM_\Delta, \quad (4)$$

where the fraction $\frac{dN_{\Delta \rightarrow N e^+ e^-}(M_\Delta)}{dM} = \frac{d\Gamma_{\Delta \rightarrow N e^+ e^-}(M_\Delta)}{dM \Gamma_{\Delta 0}^{tot}}$ is the number of $e^+ e^-$ pairs per Δ resonance, invariant mass bin and event. M_Δ is the actual mass of the Δ resonance from the simulation and $\Gamma_{\Delta 0}^{tot}$ is the total decay width at the resonance pole mass. Additionally, we use the decay width into a massive (virtual) photon

$$\Gamma(M_\Delta, M) = \frac{\lambda^{1/2}(M^2, m_N^2, M_\Delta^2)}{16\pi M_\Delta^2} m_N [2\mathcal{M}_t(M, M_\Delta) + \mathcal{M}_l(M, M_\Delta)]. \quad (5)$$

The function λ is defined by $\lambda(m_A^2, m_1^2, m_2^2) = (m_A^2 - (m_1 + m_2)^2)(m_A^2 - (m_1 - m_2)^2)$. The corresponding matrix elements \mathcal{M}_t and \mathcal{M}_l are taken from [12].

2.2. Direct Decay

The decay of a neutral vector meson in an $e^+ e^-$ -pair is a true two-body decay. Thus, energy and momentum conservation leads to the fact that the mass of the original meson (and the virtual photon) is the same as the invariant mass of the dilepton ($m_V = M_{e^+ e^-}$). For a direct decay the branching ratio reads [11] $BR(V \rightarrow e^+ e^-) = \frac{\Gamma_{V \rightarrow e^+ e^-}(M)}{\Gamma_{tot}}$ with $V = \rho^0, \omega, \phi$. $\Gamma_{V \rightarrow e^+ e^-}$ varies with the dilepton mass like M^{-3} according to [13]

$$\Gamma_{V \rightarrow e^+ e^-}(M) = \frac{\Gamma_{V \rightarrow e^+ e^-}(m_V)}{m_V} \frac{m_V^4}{M^3} \sqrt{1 - \frac{4m_e^2}{M^2}} \left(1 + 2\frac{m_e^2}{M^2}\right) \quad (6)$$

with $\Gamma_{V \rightarrow e^+ e^-}(m_V)$ the partial decay width at the resonance peak mass. For each meson mass the branching ratio (BR) is calculated and summed over in each mass bin ΔM to get the distributions dN/dM for the figures shown below.

The present calculations do not consider contributions from bremsstrahlung, because of the relatively small rates [14].

2.3. Implementation into the Simulation

In order to extract the dilepton abundances from the UrQMD model [8, 9], we use the lifetimes and 4-momenta of the calculation for each channel. A meson can be produced via the decay of a meson or baryon resonance, annihilation or string fragmentation. Such a meson obtains its mass according to the relativistic Breit-Wigner distribution, and a 4-momentum vector resulting from the kinematics in the single process under consideration. After the creation, the meson is assumed to travel on a straight line until it decays or it collides with another particle and its 4-momentum changes.

The most time consuming factor with the numerical analysis of electromagnetic processes is the suppression by a factor of $\alpha^2 \approx 10^{-5}$ due to the electromagnetic coupling. Therefore, we assume that the vector mesons radiate dileptons continuously during their whole lifetime (“shining” method). After the global freeze-out time t_f , the dilepton yield can be treated as in [12] and [15] and we get

$$\frac{dN_{e^+e^-}}{dM} = \int_0^{t_f} dt \frac{dN_V(t)}{dM} \Gamma_{V \rightarrow e^+e^-}(M) + \frac{\Gamma_{e^+e^-}(M)}{\Gamma_{tot}^V(t_f)} \frac{dN_V(t_f)}{dM}. \quad (7)$$

The second term of Eq. (7) describes the process very well if the decay rates do not depend on time. The invariant mass distribution of the dileptons is then equal to the distribution of the meson (V) itself multiplied with the branching ratio. But in a time dependent simulation one has to consider collisional broadening, i.e., the fact that the dilepton can be reabsorbed before it decays. This means that the lifetime τ of the vector meson producing the lepton pair and the decay width Γ varies for each considered hadron. In this case it is more suitable to use the time integration method.

3. Dilepton Yields at SIS Energies

In this section we present predictions for dilepton spectra which correspond to the experimental runs carried out by the HADES collaboration [16]. We consider minimum bias ($b \leq 4.5$ fm) C+C collisions at 2 AGeV. For the calculation we utilise the UrQMD model. To achieve better statistics, we randomly create 1 to 100 dilepton pairs per hadron decay (depending on hadron species and original abundances) with the direction and momenta of the dileptons in the local rest frame of each hadron. These e^+e^- momenta are transformed to the laboratory frame. For convenience, all spectra are then normalised to the mean pion multiplicity $\langle N_{\pi^0} \rangle$.

The left hand side of Fig. 1 depicts the invariant dilepton mass spectra of C+C collisions at 2 AGeV. The pion multiplicity obtained from the UrQMD calculation is $\langle N_{\pi^0} \rangle = 1.223/\text{event}$. One observes that for masses below 110 MeV the π^0 -Dalitz decay contribution is up to two magnitudes higher than the other contributions but does not account for higher masses. The Δ - and η -Dalitz decay outweigh the other yields until 400 MeV. For masses from 400 to 600 MeV the ω -Dalitz and direct ρ

decay contributions become important. The direct decays of the ρ and also that of the ω are responsible for the yields with the highest masses up to 1 GeV.

We include the coupling of the ρ meson to pions and baryons via the employed

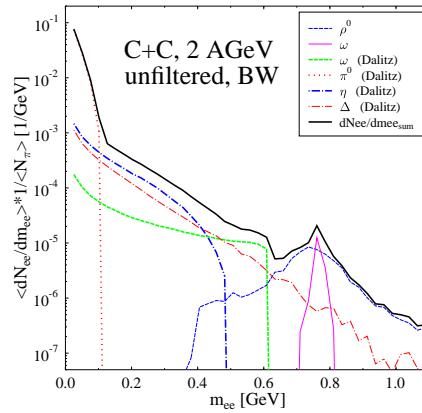
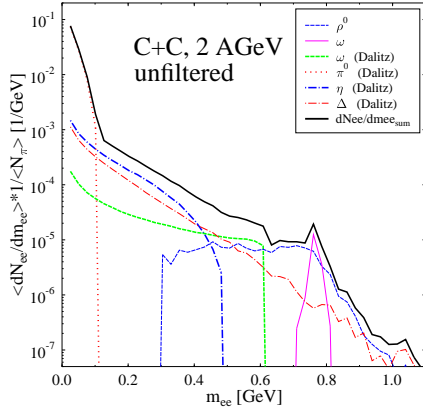


Fig. 1. Invariant mass spectra for dilepton abundances in minimum bias C+C collisions at 2 AGeV (left). The yields are normalised to the pion multiplicity $\langle N_{\pi^0} \rangle = 1.223/\text{event}$. In the right panel the ρ meson is distributed via a free Breit-Wigner distribution.

cross sections fitted to available data or calculated from detailed balance [8, 9]. In

the intermediate-mass region around 500 to 600 MeV the ρ spectrum is enhanced due to the decay chain $N^*(1520) \rightarrow N + \rho$; $\rho \rightarrow e^+e^-$. For higher ρ masses heavier baryon resonance decays and pion-pion annihilation are the most contributing parts to the spectrum. This leads to a small second hump in the dilepton spectrum. One hump is centered around 500 to 600 MeV and one at the ρ meson vacuum mass ($m_\rho = 770$ MeV).

Although the present calculation is based on vacuum cross sections and vacuum hadron widths the spectra from this many body dynamics look like what is expected from calculations employing in-medium spectral functions explicitly [5]. Due to the decay kinematics of the production channel of the ρ meson a strong modification of the ρ spectral function occurs. This effect is of kinematic origin only and will be discussed in the following section.

To investigate the difference between the ρ meson distribution originating from the UrQMD simulation with all the kinematics applied and the vacuum one, we compare now the spectra above to the case that the ρ mass has a free Breit-Wigner distribution. Figure 1 (right) depicts this scenario, the other rates remain unaltered. The discrepancy is obvious: The low-mass part of the ρ is suppressed whereas masses over 900 MeV appear. Additionally, a clear maximum around the ρ vacuum mass of 770 MeV is visible. This leads to a dip in the sum of all rates around 600 MeV. The original UrQMD spectra, in contrast, show no maximum at the vacuum mass. It is an approximately flat curve for 2 AGeV. In conclusion, the present transport model simulations suggest strong kinematic effects and leads in fact to modifications of the ρ mass spectrum and dilepton spectra.

Fig. 2 depicts invariant dilepton mass spectra from C+C collisions at 2 AGeV corrected to the HADES acceptance. The calculated dilepton momentum vectors were filtered by the HADES collaboration (the official version of the HADES acceptance filter, release 1.0, was used). This filter contains an acceptance matrix for each point at full solid angle and a smearing of the momenta according to experimental resolution.

4. ρ meson contributions

Let us finally discuss the ρ meson contributions to the dilepton spectrum. Fig. 3 depicts the ρ meson mass spectrum for minimum bias C+C reactions at 2 AGeV beam energy. One observes a double peak structure, where the peak at ~ 500 MeV originates from $N^*(1520)$ resonance decays, i.e., by the decay chain $N^*(1520) \rightarrow N + \rho$. As seen in Fig. 3 ρ mesons originating from such a baryon resonance decay have masses below 600 MeV. This effect is of kinematic nature only, since the calculation does not make use of explicit in-medium spectral functions. ρ mesons originating from $\pi\pi$ annihilation or higher mass baryon resonance decays have a mass, which is compatible with the pole mass of 770 MeV. Note that the ρ production is dominated

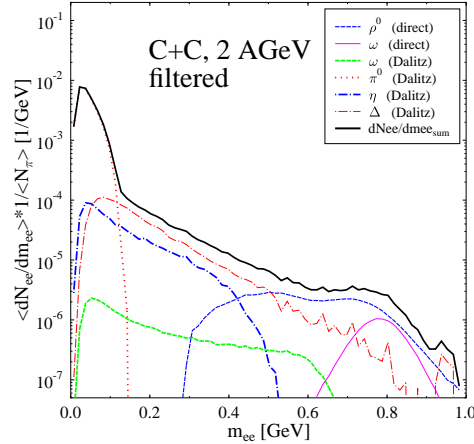


Fig. 2. Invariant mass spectrum for dilepton production in minimum bias C+C collisions at 2 AGeV. The yields are filtered by the acceptance matrix of the HADES collaboration, release 1.0.

by the decay of baryonic resonances. Direct ρ production from $\pi\pi$ scattering yields only a small contribution up to 20 % at the ρ -peak mass. For more details regarding ρ mesons in C+C collisions at 2 AGeV beam energy, the reader is referred to [17].

5. Conclusions

We have shown that due to the collision kinematics the mass spectrum of vector mesons, especially of the ρ , is modified. Therefore, a many body transport approach without explicit use of in-medium spectral functions leads to sizeable shifts in the dilepton mass distribution compared to a vacuum baseline. The prediction of a kinematically induced mass shift at 2 AGeV beam energy can be tested by the HADES experiment, e.g. when going towards target/projectile rapidities.

Acknowledgments

This work has been supported by BMBF, DFG and GSI. Fruitful discussions with Christian Sturm, Joachim Stroth and Horst Stöcker are gratefully acknowledged. Computational resources have been provided by the Center of Scientific Computing (CSC) at Frankfurt am Main.

References

1. G. E. Brown and M. Rho, Phys. Rev. Lett. **66** 2720 (1991)
2. R. Rapp and J. Wambach, Adv. Nucl. Phys. **25** 1 (2000)

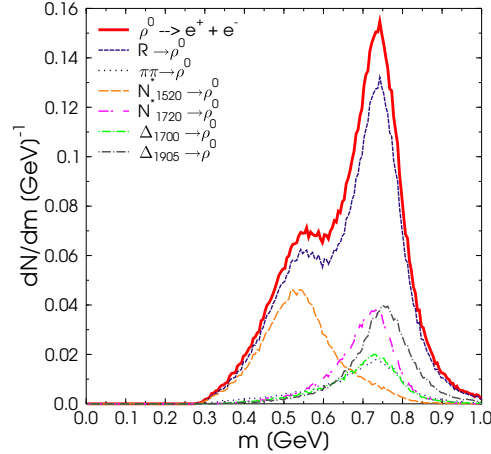


Fig. 3. Mass distribution for ρ^0 mesons for minimum bias C+C reactions at 2 AGeV. The peak around 500 MeV is due to a strong contribution from $N_{1520}^* \rightarrow p + \rho$ which amounts to 75% for masses below 600 MeV. The full line depicts the mass distribution of all decayed ρ mesons. The dashed line right below the full line depicts the ρ mesons originating from resonance decays, whereas the dotted line depicts the ρ mesons originating from $\pi\pi$ annihilation. The dashed line centered around ~ 500 MeV depicts the ρ mesons originating from $N^*(1520)$ decays.

3. W. Cassing and E. L. Bratkovskaya, Phys. Rept. **308**, 65 (1999)
4. K. Shekhter, C. Fuchs, A. Faessler, M. Krivoruchenko and B. Martemyanov, Phys. Rev. C **68** 014904 (2003)
5. M. D. Cozma, C. Fuchs, E. Santini and A. Faessler, PLB in print arXiv:nucl-th/0601059.
6. R. Schicker *et al.*, Nucl. Instrum. Meth. A **380** (1996) 586
7. C. Sturm *et al.* [KaoS Collaboration], Phys. Rev. Lett. **86** 39 (2001)
8. S. A. Bass *et al.*, Prog. Part. Nucl. Phys. **41**, 225 (1998)
9. M. Bleicher *et al.*, J. Phys. G **25** 1859 (1999)
10. L. G. Landsberg, Phys. Rept. **128**, 301 (1985)
11. P. Koch, Z. Phys. C **57**, 283 (1993)
12. G. Wolf, G. Batko, W. Cassing, U. Mosel, K. Niita and M. Schaefer, Nucl. Phys. A **517**, 615 (1990)
13. C. M. Ko, G. Q. Li, G. E. Brown and H. Sorge, Nucl. Phys. A **610**, 342C (1996)
14. C. Ernst, S. A. Bass, M. Belkacem, H. Stoecker and W. Greiner, Phys. Rev. C **58**, 447 (1998)
15. U. W. Heinz and K. S. Lee, Nucl. Phys. A **544**, 503 (1992)
16. HADES collaboration, publication in preparation, PRL to be submitted.
17. S. Vogel and M. Bleicher, Phys. Rev. C **74** 014902 (2006)